Ab Initio Study of Photochemical Reactions of Ammonia Dimer Systems

Jong Keun Park*

Department of Chemistry, Pusan National University, Pusan 609-735, Korea

Suehiro Iwata

Institute for Molecular Science, Myodaiji, Okazaki 444, Japan

Received: December 6, 1996; In Final Form: March 4, 1997[⊗]

Potential energy surfaces of ammonia dimer systems corresponding to the proton (hydrogen) transfer reaction from the reactant ($NH_3 + NH_3$) to the product ($NH_4 + NH_2$) have been calculated with ab initio HF, MP2, and SECI methods using a TZP basis set including diffuse Rydberg basis functions. The reaction path surfaces of the neutral, excited, and cationic states each have one local minimum corresponding to complexes such as (NH_3···NH_3) for a neutral one, (H_3N^*−H···NH_2) for an excited one, and (H_3N^+−H···NH_2) for a cation, respectively. Dimer complexes such as (H_3N−H···NH_2) and (H_3N···H−N^+H_2) do not exist. The photoionization and -dissociation reactions take place along the potential energy surfaces of the neutral, excited, and cationic states. The binding energies of the complexes relative to the asymptote are small. Particularly, the binding energies of H_3N^*−H···NH_2 ($^1A''$) and (H_3N···NH_3) are only 0.24 and 0.16 eV, respectively. And the head-to-head type [(H_3N···NH_3)$^+$] with a binding energy of 1.52 eV does not exist on the proton-transfer reaction surfaces.

1. Introduction

Recently, experiments involving protonated and unprotonated ammonia clusters have been extensively performed.[1−16] The photoionization mechanisms of ammonia clusters have been investigated by the various experimental techniques, such as single photon[1−4] and multiphoton[5−13] ionization and electron impact methods.[14−16] The protonated cluster ions [$(NH_3)_nH^+$] are found to be produced by two main steps.[7,11,12] In the first one, the excited ammonia clusters $(NH_3)_{n-2}(H_3N^*-H\cdots NH_2)$ are formed from the predissociative state of the ammonia molecule in the cluster through the multiphoton absorption process. In the second one, the species $(NH_3)_{n-2}$ (H_3N^*−H···NH_2) releases an electron to produce the cluster ions, and then it is divided into the protonated ion and NH_2 through a proton-transfer reaction, while the unprotonated ion [$(NH_3)_n^+$] is produced via absorption of a single photon or electron impact and subsequent release of an electron.[4,14]

Potential energy curves of protonated ammonia cluster ions via the multiphoton ionization mechanism have been constructed by Castleman et al.[12,13] According to these potential energy curves, an electron is released by the multiphoton ionization process and the unprotonated cluster ions [$(NH_3)_n^+$] dissociate into $(NH_3)_{n-1}H^+ + NH_2$ along the cationic potential curves. The $(NH_3)_n^+$ and [$(NH_3)_{n-1}H^+ + NH_2$] species have local minima with an energy barrier. Very recently, these authors also measured experimentally the peaks of unprotonated cluster ions [$(NH_3)_n^+$, $n = 2-5$]. The peaks of these unprotonated ions are very weak compared to the protonated ions.

In another experiment, Fuke et al.[17] have suggested that protonated ammonia clusters can also be produced as a new photolysis product in the form of $(NH_2\cdots NH_4)^*(NH_3)_{n-2}$. The intermediate $(NH_2\cdots NH_4)^*(NH_3)_{n-2}$ is formed through a cage dynamics of the predissociation of large clusters. In this experiment, the protonated ion $(NH_2\cdots NH_4^+)(NH_3)_{n-2}$ has been observed by single photon ionization of an intermediate having an ionization threshold of 3.79 eV.

It is worth noting that the theoretically adiabatic ionization energies for the unprotonated ammonia dimer cations are 8.5[18] and 7.71 eV,[19] while the vertical energy is 9.15 eV.[19] The experimental vertical energies are 9.54[1] and 9.19 eV.[4]

Although the photoionization process of the ammonia clusters has already been studied by various methods, further investigations seem to be worth carrying out on the basis of the following points. (i) In the dimer cation, does the head-to-head cationic complex ($H_3N\cdots NH_3)^+$ dissociate into ($NH_4^+ + NH_2$) along the proton-transfer reaction surface? That is, does the intermediate complex exist? (ii) Does a cage species $(NH_2\cdots NH_4)^*$ obtained as an intermediate of the intracluster reactions exist? (iii) Why were the unprotonated ammonia cluster ions [$(NH_3)_n^+$] observed to be very weak except for $n = 1$ and 2? (iv) In the ammonia dimer cation, what is the reason for the ionization energy gap between the theoretical and experimental values? Answers to these questions concerning a detailed understanding of the photoionization processes clearly require state-to-state correlation surfaces of the ground, excited, and cationic states between the reactant species ($NH_3 + NH_3$) and the products ($NH_4 + NH_2$).

In this work, we have studied state-to-state correlation curves of the ground, excited, and cationic states from the reactant asymptote ($NH_3 + NH_3$) to product ($NH_4 + NH_2$) in order to obtain the relative energy gap and local intermediate complexes along the proton (hydrogen) transfer reaction paths. The protonated ammonia dimer cation is found to be produced from the excited complex of the hydrogen-bonded type by the absorption ionization dissociation [AID] or absorption dissociation ionization [ADI] mechanisms. Since studies of the mechanisms involving the unprotonated dimer cation seem to be quite limited theoretically and experimentally, we have also examined the ionization process of the nonhydrogen-bonded dimer cation ($H_3N\cdots NH_3)^+$, which has a head-to-head type interaction. We show that the head-to-head interaction dimer cation plays an important role in the photoionization process of the unprotonated ammonia dimer cation. In addition, the photodissociation reactions of the NH_4 radical are examined as a fundamental

[⊗] Abstract published in *Advance ACS Abstracts,* April 1, 1997.

S1089-5639(96)04000-5 CCC: $14.00

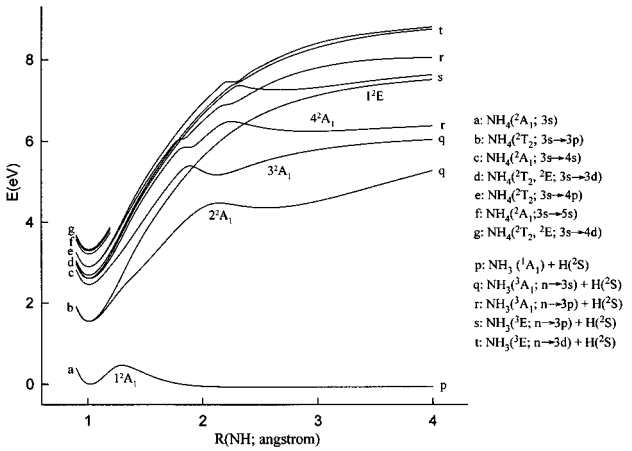

Figure 1. Potential energy curves for the ground and excited states of the NH_4 Rydberg radical dissociating into (NH_3 + H).

unit in photochemical processes of $(NH_3)_n$ clusters. Our results are also compared with the experimental[20−22] and other theoretical[23−33] values.

2. Calculational Methods

The basis sets chosen are the triple-ζ basis on N (521/2111)[45] and H(511).[46] Two extra d type polarization functions[45] are added to nitrogen (α_d = 0.412, 1.986) and one extra p type function to hydrogen (α_p = 0.990 495). The diffuse Rydberg basis functions (α_s = 0.028, 0.0066; α_p = 0.025, 0.0051; α_d = 0.015, 0.0032)[47] are additionally augmented on nitrogen to describe the Rydberg states of NH_3 and NH_4. The total number of contracted basis set used in ammonia dimer is 130.

The geometric structures of the ammonia monomer, dimers, and their cations are optimized with the MP2 (second-order Möller Plesset) approximation using Gaussian 92. The potential energy surfaces of the proton-transfer reaction from (NH_3 + NH_3^+) to (NH_4^+ + NH_2) via a complex (H_3N^+−H···NH_2) is calculated with the UHF wave functions for R_{NN} and r_{NH} by optimizing the other geometric parameters.

The excited states of NH_3, $(NH_3)_2$, and NH_4 are somewhat of a Rydberg nature with a cationic core. The ground state of NH_4 itself is often called the Rydberg radical. Therefore, the geometric structures of these states are expected to be similar to those of the corresponding cations. To draw the potential energy curves and surfaces, we use the characteristics of the states twofold. The geometry of the corresponding cation is assumed in drawing the potential energy curves for the dissociation of the ground and excited states of NH_4 to (NH_3 + H) and for the hydrogen transfer reactions of (NH_3 + NH_3*) to (NH_4* + NH_2) via a complex (H_3N^*−H···NH_2). Besides, the molecular orbitals for the configuration interaction (CI) are determined with the open shell restricted Hartree−Fock method for the corresponding cation. The SECI (singly excitation configuration interaction) method is used for the potential energy calculations.

To examine the appropriateness of the procedure, the potential energies of the ground-state surface from NH_4 to (NH_3 + H) have been calculated with the SDCI and CCSD(T) methods. In the SDCI and CCSD(T) calculations an f type basis function (α_f = 1.093)[48] is added to the above basis set.

3. Results and Discussion

The potential energy curves for the ground and low lying excited states of the NH_4 Rydberg radical dissociating into (NH_3 + H) are drawn in Figure 1. Because of the complexity, we have cut the potential energy curves of the high-lying excited states at R_{NH} =1.2 Å and have not connected the curves between R_{NH} = 4.0 Å and the asymptote (NH_3 + H). The $^2A_1$ ground state of the NH_4 radical correlates with the asymptote (NH_3 + H). The ground state is metastable, and the potential well is shallow. Although the ground state of the NH_4 radical has an energy barrier of 0.6 eV along the NH bond rupture, the stability of the NH_4 radical seems to be influenced by tunneling. The existence of the NH_4 radical has been confirmed by the solvated electron reaction and by electrochemical approaches.[34−37] The lifetime of the NH_4 radical was measured experimentally to be 13 ps, a value more than 10^6 times shorter than in the one for NH_4 in ammonia clusters.[17]

The equilibrium and transition state distances and the relative energies of the NH_4 radical dissociating into (NH_3 + H) are listed in Table 1 together with the ionization and excitation energies of the ammonia molecules. All energies are adiabatic values. The excitation energies of the ammonia molecules [NH_n (n = 2−4)] calculated by the SECI method are in reasonable agreement with the experimental[20−23] and theoretical[24,26,27] values.

The NH equilibrium internuclear distance of ∼1.04 Å is larger than that (R_{NH} = 1.012 Å) of a monomer NH_3, since in its ground state the NH_4 radical has an electron in a 3s Rydberg orbital, that is, NH_4 is a semi-ionic state.

At the transition state the bond length (R_{NH}) is ∼1.43 Å, that is, the bond breaking in NH_4 takes place near the equilibrium geometry. Therefore, the NH_4 radical has the weak NH bonds. The energy barriers of the NH_4 and (NH_3 + H) to the transition state are ∼0.8 and ∼0.6 eV, respectively. In the excitation energy of the NH_4 radical, our results are similer to the other theoretical[24,26,27] and experimental[21,22] results.

State-to-state correlation diagrams of the ground, excited, and cationic state surfaces correlating the dimer reactant asymptote (NH_3 + NH_3) and the product asymptote (NH_4 + NH_2) are drawn in Figure 2. All energy gaps are adiabatic. The potential energy of the ammonia dimer is set equal to zero. The complexes and the asymptotes are connected with dotted lines. The ammonia dimer complexes on these surfaces correspond to NH_3···NH_3, H_3N^*−H···NH_2, and H_3N^+−H···NH_2 for the neutral, the excited, and the cationic complexes, respectively.

Similar to previous results,[38−44] we also found that the structure of the dimer is not a hydrogen-bonded type complex. The floppy nature of this complex can be associated with three motions, that is, internal rotation of each monomer, interchange tunneling, and inversion tunneling of each monomer.

The N···H internuclear distance of the dimer calculated with the MP2 method is 2.306 Å. The R_{NN} distance in this work and the experimental[40] one are 3.326 and 3.337 Å, respectively. The binding energies of the ammonia dimer complex (NH_3···NH_3) from the asymptotes (NH_3 + NH_3) and (NH_4 + NH_2) are 0.16 and 4.87 eV, respectively. From the complex (NH_3···NH_3) to the asymptote (NH_4 + NH_2), the hydrogen transfer reaction takes place through the ground-state surface. We could not find the local minimum of a complex such as (H_3N−H···NH_2) on the surface.

On the first excited-state surface correlating [NH_3 + NH_3*($^1A_1$)] to [NH_4 + NH_2*($\tilde{A}^2A_1$)], our local minimum corresponds to an excited complex (H_3N−H···NH_2)*($^1A'$). From the complex (H_3N−H···NH_2)* to the asymptotes (NH_3 + NH_3*) and (NH_4 + NH_2*), the hydrogen transfer reaction also takes place through the excited-state surface. The binding energies of this excited complex from the asymptote [NH_4 + NH_2*($\tilde{A}^2A_1$)] and [NH_3 + NH_3*($^1A_1$)] are 0.75 and 0.95 eV, respectively. The

TABLE 1: Relative Energies (eV) for the $^2A_1$ Ground States along the NH_4 Radical Dissociating into $NH_3 + H^o$

	SECI[a]	QDCI[b]	CCSD(T)[c]	CIPSI[d]	SDCI[e]	exptl[f]
$R(NH)_{eq}$[g]	1.022	1.040	1.040	1.033	1.041	
$R(NH)_{TS}$[g]	1.339	1.439	1.425	1.369	1.427	
$\Delta E_{[TS-(NH_3+H)]}$	0.59	0.61	0.57	0.52	0.64	
$\Delta E_{[NH_4-(NH_3+H)]}$	−0.17	−0.22	−0.22	−0.23	−0.21	−0.3[h]
$\Delta E_{(NH_4-TS)}$	0.75	0.83	0.79	0.88	0.85	
NH_4						
IE[i]			4.60			4.62[k]
$\Delta E_{(3s-3p)}$	1.55	1.90		1.66	1.89	
$\Delta E_{(3s-4s)}$	2.46	2.78		2.65		
$\Delta E_{(3s-3d)}$; $^2T_2$	2.61	2.99			2.89	2.18[l]
$\Delta E_{(3s-3d)}$; ^2E	2.69	3.13			3.04	
$\Delta E_{(3s-4p)}$	2.90	3.31				
$\Delta E_{(3s-5s)}$	3.22					
$\Delta E_{(3s-4d)}$; $^2T_2$	3.29					
$\Delta E_{(3s-4d)}$; ^2E	3.32					
$\Delta E_{(3p-3d)}$; $^2T_2$	1.06	1.23				1.87[l]
NH_3						
IE[j]			10.14			10.17
$\Delta E_{(n-3s)}$; $\tilde{A}^3A_1$	6.46	6.31			6.27[m]	6.38
$\Delta E_{(n-3p_{x,y})}$; $\tilde{B}^3E$	7.88	7.86			7.84[m]	7.90
$\Delta E_{(n-3p_z)}$; $^3A_1$	8.29	8.05			7.84[m]	8.14
$\Delta E_{(n-4s)}$; $^3A_1$	8.98	9.06				9.11
$\Delta E_{(n-3d)}$; ^3E	9.09					
NH_2						
$\Delta E_{(n-3s)}$; $\tilde{A}^2A_1$	1.40	1.29				1.26[n]

[a] SECI energies were obtained with the MOs and geometries of NH_4^+ calculated by RHF at each internuclear distance. [b] QDCI energies were obtained with a suite of MOLYX. [c] CCSD(T) energies were obtained with Gaussian 92. [d] Reference 27. [e] Reference 26. [f] Reference 20. [g] Unit of internuclear distance is angstrom. [h] Cited from ref 27. [i] Ionization energy of NH_4 is optimized with MP2 calculations. [j] Ionization energy of NH_3 is optimized with MP2 calculations. [k] Reference 21. [l] Reference 22. [m] Reference 24. [n] Reference 23. [o] All energies are adiabatic values.

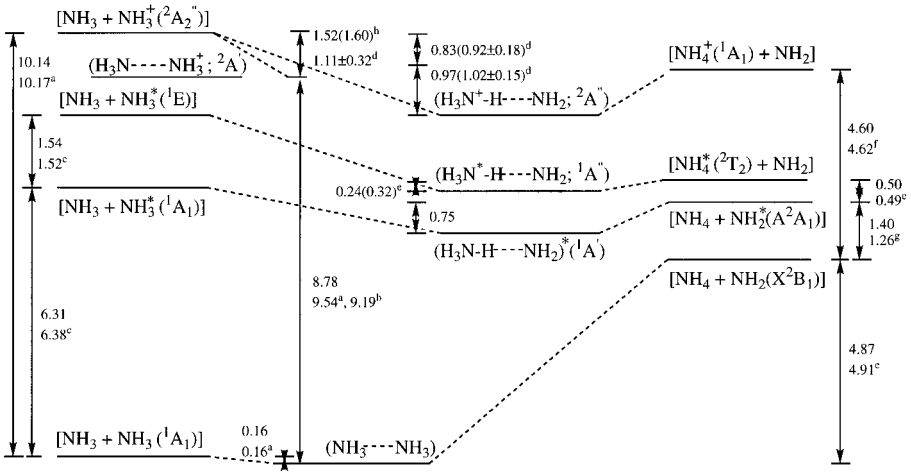

Figure 2. Schematic energy diagram of the hydrogen and proton transfer surfaces from the asymptote ($NH_3 + NH_3$) to ($NH_4 + NH_2$), and relative energies of the neutral, excited, and cationic complexes. All energies are adiabatic values and are in units of eV. Superscripted letters indicate data from the following sources: (a) ref 1; (b) ref 4; (c) ref 20; (d) ref 16; (e) ref 18; (f) ref 17; (g) ref 23; (h) ref 28.

energy gaps of $(H_3N-H\cdots NH_2)^*$ relative to $(H_3N^+-H\cdots NH_2; {}^2A'')$ and $(NH_3\cdots NH_3)$ are ∼2.93 and ∼5.52 eV, respectively.

We note that Fuke et al.[17] have found a cage product in the predissociation process of large ammonia clusters and assigned it as an excited-state $(NH_4^*\cdots NH_2)(NH_3)_{n-2}$. An ionization threshold of 3.79 eV by a single photon mechanism from this complex has been observed. This ionization threshold is larger than our energy gaps of 2.93 eV. Therefore, the cage complex is different from the first excited-state $(H_3N-H\cdots NH_2)^*({}^1A')$.

The potential energy surface of the reaction $[(NH_3 + NH_3^*; {}^1A_1), A] \rightarrow [(H_3N-H\cdots NH_2)^*({}^1A'), B] \rightarrow [(NH_4 + NH_2; \tilde{A}^2A_1), C]$ is presented in Figures 3 and 4. The contour map drawn corresponds to potential energies for internuclear distances ranging from 2.4 to 3.4 Å for NN and from 0.7 to 2.7 Å for NH. To understand easily the reaction path surface, we have just represented A and C on Figures 3 and 4. A and C are not the positions of the asymptotes. A circle near A is an artifact caused by the fitting procedure of the potential energy curves. This contour map has a local minimum point at B. The distances of R_{NN} and r_{NH} at B are 3.09 and 1.07 Å, respectively. Figure 4 is drawn by cutting the vertical axis of Figure 3.

The second excited complex $(H_3N^*-H\cdots NH_2; {}^1A'')$ correlates with $[NH_4^*({}^2T_2) + NH_2(X^2B_1)]$. From the complex $(H_3N^*H\cdots NH_2)$ to the asymptotes $(NH_3 + NH_3^*)$ and $(NH_4^* + NH_2)$, the proton and charge transfer reactions take place through the excited-state surface. This excited complex had been found to be formed by a predissociative reaction $(NH_3 \rightarrow NH_2 + H)$ of the ammonia monomer in the ammonia clusters via an intracluster reaction. The binding energy of this state relative to the asymptote $[NH_4^*({}^2T_2) + NH_2(X^2B_1)]$ is 0.24 eV. The potential well is very shallow. Thus, the complex $(H_3N^*-H\cdots NH_2)$ is easily dissociated into $NH_4^* + NH_2$. The energy gaps of $(H_3N^*-H\cdots NH_2; {}^1A'')$ relative to $(H_3N^+-H\cdots NH_2; {}^2A'')$ and $(NH_3\cdots NH_3)$ are ∼1.92 and ∼6.53 eV, respectively.

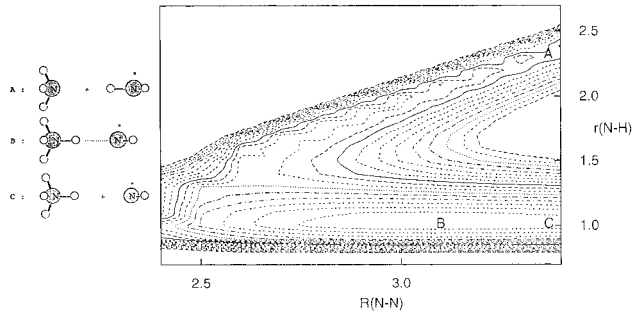

Figure 3. Energy contour map of the hydrogen transfer surface covering the reactant [$NH_3 + NH_3^*(^1A_1)$, A], the complex [$(H_3NH\cdots NH_2)^*(^1A')$, B], and the asymptote [$NH_4 + NH_2(\tilde{A}^2A_1)$, C]. The energy difference between the neighboring isoenergetic lines is 0.112 eV. A and C are not the exact positions of the asymptotes.

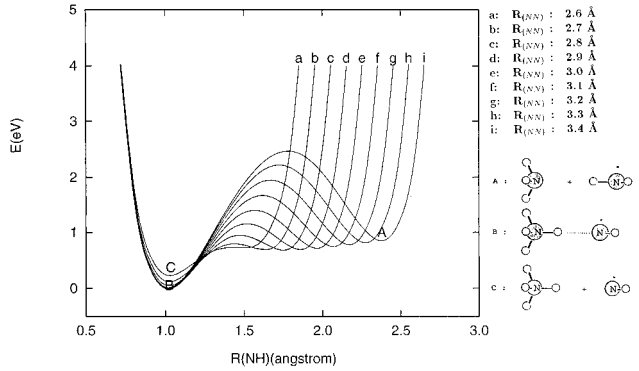

Figure 4. Reaction path surface of the hydrogen transfer reaction covering the reactant [$NH_3 + NH_3^*(^1A_1)$, A], the complex [$(H_3NH\cdots NH_2)^*(^1A')$, B], and the asymptote [$NH_4 + NH_2$ ($\tilde{A}^2A_1$), C].

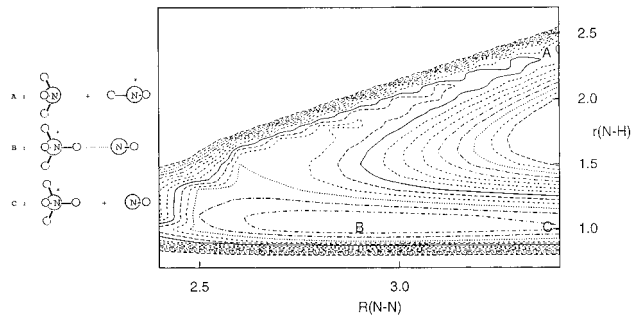

Figure 5. Energy contour map of the proton (charge) transfer surface covering the reactant [$NH_3 + NH_3^*(^1E)$, A], the complex [$(H_3N^*H\cdots NH_2$; $^1A''$), B], and the asymptote [$NH_4^*(^2T_2) + NH_2(X^2B_1)$, C]. The energy difference between the neighboring isoenergetic lines is 0.1299 eV. A and C are not the exact positions of the asymptotes.

We have also calculated the second excited potential energy surface of the reaction [$NH_3 + NH_3^*(^1E)$, A] → [$(H_3N^*-H\cdots NH_2$; $^1A''$), B] → [$NH_4^* + NH_2(X^2B_1)$, C], which is shown in Figures 5 and 6. The contour map drawn corresponds to potential energies for internuclear distances ranging from 2.4 to 3.4 Å for NN and from 0.7 to 2.7 Å for NH. To understand easily the reaction path surface, we have just represented A and C on Figures 5 and 6. A and C are not the positions of the asymptotes. B is a minimum complex ($H_3N^*-H\cdots NH_2$; $^1A''$) at this surface. The potential energy increases directly from B to A and C. The R_{NN} and r_{NH} at B are 2.93 and 1.03 Å, respectively. Figure 6 is drawn by cutting the vertical axis of Figure 5. The energy gap between B and C is small, and this excited complex is slightly unstable. Therefore, in the process of producing the protonated ammonia cluster cation, the competing process between the photon absorption−ionization−dissociation (AID) and the photon absorption−dissociation−ionization (ADI) mechanism in two-photon ionization will take place. This state plays a bridge role in the resonance-enhanced multiphoton ionization mechanism.

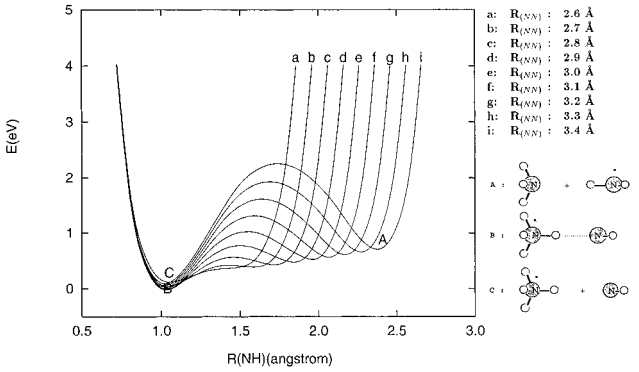

Figure 6. Reaction path surface of the proton (charge) transfer reaction covering the reactant [$NH_3 + NH_3^*(^1E)$, A], the complex [$(H_3N^*H\cdots NH_2$; $^1A''$), B], and the asymptote [$NH_4^*(^2T_2) + NH_2(X^2B_1)$, C].

There are two possible geometric structures for the dimer cation. One is a hydrogen-bonded dimer cation ($H_3N^+-H\cdots NH_2$; $^2A''$) with binding energies of 0.97 and 1.85 eV relative to the [$NH_4^+(^1A_1) + NH_2$] and [$NH_3 + NH_3^+(^2A_2'')$] asymptotes, respectively. The energy gap between this dimer cation ($^2A''$) and the second excited complex ($H_3N^*-H\cdots NH_2$; $^1A''$) is 1.92 eV, and the ionization energy of this complex relative to the neutral dimer ($NH_3\cdots NH_3$) is 8.45 eV. Ionization energy of 8.5 eV for the unprotonated ammonia dimer cations suggested by Kassab et al.[18] is similar to ours. Therefore, they might have calculated the ionization energy of the hydrogen-bonded type dimer cation ($H_3N^+-H\cdots NH_2$; $^2A''$).

The other is a head-to-head interaction $(H_3N\cdots NH_3)^+$ (D_{3d} symmetry), which is formed by the interaction between the dipole moment and the cationic charge. According to the geometric structure of this complex, the ionization of the NH_3 occurs with the single photon, and NH_3^+ combines with NH_3. The ionization energy of this cation relative to ($NH_3\cdots NH_3$) is 8.78 eV. The binding energy of $(H_3N\cdots NH_3)^+$ with respect to ($NH_3 + NH_3^+$) is 1.52 eV. The potential energy of ($H_3N\cdots NH_3$)$^+$ is higher than that of $(H_3N^+-H\cdots NH_2)$.

The cationic potential energy surfaces for the proton-transfer reaction [$NH_3 + NH_3^+(^2A_2'')$, A] → [$H_3N^+-H\cdots NH_2$; $^2A''$), B] → [$NH_4^+(^1A_1) + NH_2(X^2B_1)$, C] are drawn in Figures 7 and 8. The contour map drawn corresponds to potential energies for internuclear distances ranging from 2.4 to 3.6 Å for NN and from 0.7 to 2.9 Å for NH. To understand easily the reaction path surface, we have just represented A and C on Figures 7 and 8. A and C are not the positions of the asymptotes. B is only a local minimum point in this potential energy surface. The optimized distances R_{NN} and r_{NH} at B are 2.87 and 1.04 Å, respectively. A small circle near A is an artifact caused by the fitting procedure. The potential curve increases stiffly from B to A. The binding energy between B and C is slightly larger than those of the excited states. The contour map of the dimer cation is very similar to that of the excited molecule. Figure 8 was drawn by cutting the vertical axis of Figure 7. In Figure 8, B is also represented as a minimum point. Because Figure 8 was drawn with potential energies for R_{NN} ranging from 2.6 to 3.6 Å, the energy gaps of B relative to A and C are different from that of Figure 7.

We note that Castleman et al.[13] observed very weak peaks of the unprotonated ammonia cluster [$(NH_3)_n^+$ ($n = 2-5$)] using the multiphoton ionization method[13] and drew a schematic diagram of the potential energy curves during multiphoton ionization of the protonated ammonia clusters.[12] The peaks of

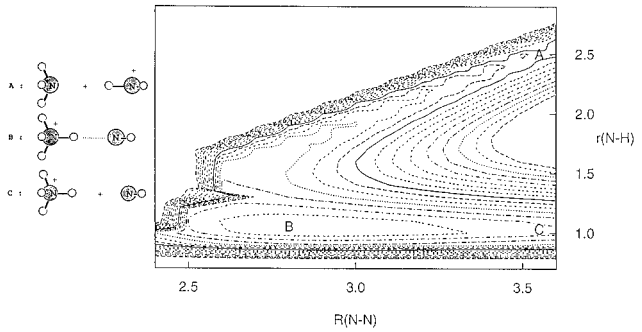

Figure 7. Energy contour map of the proton transfer surface covering the reactant [$NH_3 + NH_3^+(^2A_2'')$, A], the complex [$(H_3N^+H\cdots NH_2$; $^2A''$), B], and the asymptote [$NH_4^+(^1A_1) + NH_2(X^2B_1)$, C]. The energy difference between the neighboring isoenergetic lines is 0.10 eV. A and C are not the exact positions of the asymptotes.

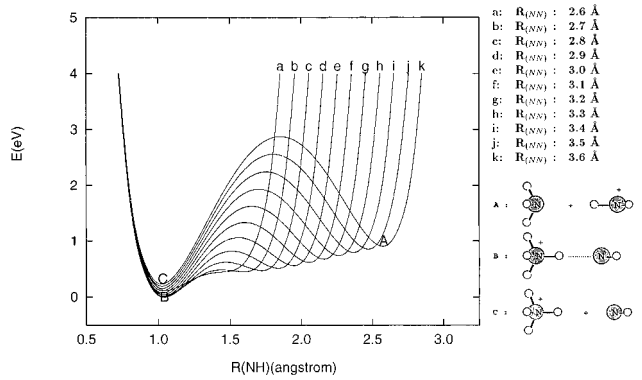

Figure 8. Reaction path surface of the proton transfer reaction covering the reactant [$NH_3 + NH_3^+(^2A_2'')$, ***A***], the complex [$(H_3N^+H\cdots NH_2$; $^2A''$), B], and the asymptote [$NH_4^+(^1A_1) + NH_2(X^2B_1)$, C].

the unprotonated ammonia clusters were very weak except for the dimer cation. In our results, a head-to-head type dimer cation $(H_3N\cdots NH_3)^+$ does not exist on the proton transfer reaction surfaces from the reactant to the product. The protonated and unprotonated clusters have two local minima by an energy barrier of 0.45 eV. The energy gap between the two isomers is 0.33 eV. The head-to-head type structure might contribute to the peak of the unprotonated dimer cation with a binding energy of ~1.52 eV. The geometric structure of the head-to-head is different from the protonated dimer cation (hydrogen-bonded). To change the geometric structure from the head-to-head to the hydrogen-bonded type, a monomer is rotated to the other, and a proton of the monomer transfer to the other. Because of the small energy barrier, the head-to-head complex may be transferred to the hydrogen-bonded type if the excess energy is supplied by either electron or photon excitation.

4. Conclusions

We have calculated state-to-state correlation energy curves for the hydrogen and proton transfer reactions from the reactant asymptote ($NH_3 + NH_3$) to the product ($NH_4 + NH_2$). The correlation energy curves of the neutral, excited, and cationic species have only one local minimum complex each. Each local minimum on the potential surfaces corresponds to complexes such as $(H_3N^+-H\cdots NH_2)$ for the cation, $(H_3N^*-H\cdots NH_2)$ for the excited state, and $(NH_3\cdots NH_3)$ for the neutral. But the dimer complexes such as $(H_3N-H\cdots NH_2)$, $(H_3N\cdots H-N^+H_2)$, and $(H_3N\cdots H-N^*H_2)$ have not been confirmed.

On the energy curves of the neutral and first excited states the hydrogen (atom) transfer reaction takes place. But the proton and charge transfers take place on the energy curve of the second excited state. In the cationic energy curve the proton transfer takes place.

According to the geometric structure, the head-to-head interaction dimer cation $(H_3N\cdots NH_3)^+$ does not exist on the proton-transfer reaction surfaces from the reactant ($NH_3 + NH_3^+$) to the product ($NH_4^+ + NH_2$). But the protonated dimer cation of ($H_3N^+-H\cdots NH_2$; $^2A''$) exists on the proton transfer reaction surface. The energy barrier between the two isomers is small. Therefore, the geometric change from the head-to-head to the hydrogen-bonded type takes place easily with an excess energy. The ionization energies of $(H_3N\cdots NH_3)^+$ and ($H_3N^+-H\cdots NH_2$; $^2A''$) relative to the neutral ammonia dimer are 8.78 and 8.45 eV, respectively.

The first excited state $(H_3N-H\cdots NH_2)^*(^1A')$ correlates with $[NH_4 + NH_2(\tilde{A}^2A_1)]$ including the binding energy of 0.75 eV.

The second excited state ($H_3N^*-H\cdots NH_2$; $^1A''$) correlates with $[NH_4^*(^2T_2) + NH_2]$ by its binding energy of 0.24 eV. Because of the weak binding, a competing reaction between AID and ADI takes place to produce the protonated ammonia dimer cation. These excited states play an important bridge role on the multiphoton ionization process.

Acknowledgment. The authors thank Professor Fuke and Dr. Ten-no for their valuable discussions. The Korea Science and Engineering Foundation is acknowledged for the financial support of Jong Keun Park.

References and Notes

(1) Ceyer, S. T.; Tiedemann, P. W.; Mahan, B. H.; Lee, Y. T. *J. Chem. Phys.* **1979**, *70*, 14.
(2) Shinohara, H.; Nishi, N.; Washida, N. *J. Chem. Phys.* **1985**, *83*, 1939.
(3) Kaiser, E.; de Vries, J.; Steger, H.; Menzel, C.; Kamke, W.; Hertel, I. V. *Z. Phys. D* **1991**, *20*, 193.
(4) Kamke, W.; Herrman, R.; Wang, Z.; Hertel, I. V. *Z. Phys. D* **1988**, *10*, 491.
(5) Shinohara, H.; Nishi, N. *Chem. Phys. Lett.* **1982**, *87*, 561.
(6) Shinohara, H. *J. Chem. Phys.* **1983**, *79*, 1732.
(7) Echt, O.; Dao, P. D.; Morgan, S.; Castleman, A. W., Jr. *J. Chem. Phys.* **1985**, *82*, 4076.
(8) Wei, S.; Tzeng, W. B.; Castleman, A. W., Jr. *J. Chem. Phys.* **1990**, *92*, 332.
(9) Pursell, C. J.; Weliky, D. P.; Oka, T. *J. Chem. Phys.* **1990**, *93*, 7041.
(10) Wei, S.; Tzeng, W. B.; Castleman, A. W., Jr. *J. Chem. Phys.* **1990**, *93*, 2506.
(11) Misaizu, F.; Houston, P. L.; Nishi, N.; Shinohara, H.; Kondow, T.; Kinoshita, M. *J. Chem. Phys.* **1993**, *98*, 336.
(12) Purnell, J.; Wei, S.; Buzza, S. A.; Castleman, A. W., Jr. *J. Phys. Chem.* **1993**, *97*, 12530.
(13) Buzza, S. A.; Wei, S.; Purnell, J.; Castleman, A. W., Jr. *J. Chem. Phys.* **1995**, *102*, 4832. Wei, S.; Purnell, J.; Buzza, S. A.; Castleman, A. W., Jr. *J. Chem. Phys.* **1993**, *99*, 755.
(14) Odutola, J. A.; Dyke, T. R.; Howard, B. J.; Muenter, J. S. *J. Chem. Phys.* **1979**, *70*, 4884.
(15) Stephan, K.; Futrell, J. H.; Peterson, K. I.; Castleman, A. W., Jr.; Wager, H. E.; Djuric, N.; Mark, T. D. *Int. J. Mass Spectrom. Ion Phys.* **1982**, *44*, 167.
(16) Posey, L. A.; Guettler, R. D.; Kirchner, N. J.; Zare, R. N. *J. Chem. Phys.* **1994**, *101*, 3772.
(17) Fuke, K.; Takasu, R. *Bull. Chem. Soc. Jpn.* **1995**, *68*, 3309.
(18) Cao, H. Z.; Evleth, E. M.; Kassab, E *J. Chem. Phys.* **1984**, *81*, 1512.
(19) Greer, J. C.; Ahlrichs, R.; Hertel, I. V. *Z. Phys. D* **1991**, *18*, 413.
(20) Skerbele, A.; Lassettre, E. N. *J. Chem. Phys.* **1965**, *42*, 395.
(21) Fuke, K.; Takasu, R.; Misaizu, F. *Chem. Phys. Lett.* **1994**, *229*, 597.
(22) Herzberg, G. *Faraday Discuss. Chem. Soc.* **1981**, *71* 165.
(23) Lathan, W. A.; Hehre, W. J.; Curtiss, L. A.; Pople, J. A. *J. Am. Chem. Soc.* **1971**, *93*, 6377.
(24) Runau, R.; Peyerimhoff, S. D.; Buenker, R. J. *J. Mol. Spectrosc.* **1977**, *68*, 253.
(25) Albritton, D. L. *At. Data Nucl. Data Tables* **1978**, *22*, 1.
(26) Kaspar, J.; Smith, V. H., Jr.; McMaster, B. N. *Chem. Phys.* **1985**, *96*, 81.
(27) Kassab, E.; Evleth, E. M. *J. Am. Chem. Soc.* **1987**, *109*, 1653.

(28) Amor, N. B.; Maynau, D.; Spiegelmann, F. *J. Chem. Phys.* **1996**, *104*, 4049.
(29) Tachibana, A.; Kawauchi, S.; Kurosaki, Y.; Yoshida, N.; Ogihara, T.; Yamabe, T. *J. Phys. Chem.* **1991**, *95*, 9647.
(30) Gill, P. M. W.; Radom, L. *J. Am. Chem. Soc.* **1988**, *110*, 4931.
(31) Tachikawa, H.; Tomoda, S. *Chem. Phys.* **1994**, *182*, 185.
(32) Tomoda, S.; Kimura, K. *Chem. Phys. Lett.* **1985**, *121*, 159.
(33) Bouma, W. J.; Radom, L. *J. Am. Chem. Soc.* **1985**, *107*, 345.
(34) Wan, J. K. S. *J. Chem. Educ.* **1968**, *45*, 40.
(35) Brooks, J. M.; Dewald, R. R. *J. Chem. Phys.* **1971**, *75*, 986.
(36) Kariv-Miller, E.; Nanjundiah, C.; Eaton, J.; Swenson, K. E. *J. Electroanal. Chem.* **1984**, *167*, 141.
(37) Evleth, E. M.; Kassab, E. *Pure Appl. Chem.* **1988**, *60*, 209.
(38) Snels, M.; Fantoni, R.; Sanders, R.; Weerts, W. L. *Chem. Phys.* **1987**, *115*, 79.
(39) Havenith, M.; Linnartz, H.; Zwart, E.; Kips, A.; ter Meulen, J. J.; Meerts, W. L. *Chem. Phys. Lett.* **1992**, *193*, 261.
(40) Olthof, E. T. H.; van der Avoird, A.; Wormer, P. E. S. *J. Mol. Struct.* **1994**, *307*, 201.
(41) Linnartz, H.; Meerts, W. L.; Havenith, M. *Chem. Phys.* **1995**, *193*, 327.
(42) Sagarik, K. P.; Ahlrichs, R.; Brode, S. *Mol. Phys.* **1986**, *57*, 1247.
(43) Greer, J. C.; Ahlrichs, R.; Hertel, I. V. *J. Chem. Phys.* **1991**, *95*, 3861.
(44) Greer, J. C.; Ahlrichs, R.; Hertel, I. V. *Z. Phys. D* **1991**, *18*, 413.
(45) Huzinaga, S.; Andzelm, J.; Klobukowski, M.; Radzio-Andzelm, E.; Sakai, Y.; Tatewaki, H. *Physical Science Data, Gaussian basis sets for molecular calculations*; Elsevier: Amsterdam, 1984; Vol. 16.
(46) Hasimoto, K.; Osamura, Y. *J. Chem. Phys.* **1991**, *95*, 1121.
(47) Poirier, R.; Kari, R.; Csizmadia, I. G. *Physical Science Data, Handbook of Gaussian basis sets*; Elsevier: Amsterdam, 1985; Vol. 24.
(48) Almlöf, J.; Taylor, P. R. *J. Chem. Phys.* **1987**, *86*, 4070.